Alterations of diffusion kurtosis measures in gait-related white matter in the "ON–OFF state" of Parkinson's disease

Xuan Wei[1], Shiya Wang[2], Mingkai Zhang[2], Ying Yan[1], Zheng Wang[1], Wei Wei[3], Houzhen Tuo[2], Zhenchang Wang[1]

[1]Department of Radiology, Beijing Friendship Hospital, Capital Medical University, Beijing 100050, China;
[2]Department of Neurology, Beijing Friendship Hospital, Capital Medical University, Beijing 100050, China;
[3]Division of Science and Technology, Beijing Friendship Hospital, Capital Medical University, Beijing 100050, China.

Abstract

Background: Gait impairment is closely related to quality of life in patients with Parkinson's disease (PD). This study aimed to explore alterations in brain microstructure in PD patients and healthy controls (HCs) and to identify the correlation of gait impairment in the ON and OFF states of patients with PD, respectively.

Methods: We enrolled 24 PD patients and 29 HCs from the Movement Disorders Program at Beijing Friendship Hospital Capital Medical University between 2019 and 2020. We acquired magnetic resonance imaging (MRI) scans and processed the diffusion kurtosis imaging (DKI) images. Preprocessing of diffusion-weighted data was performed with Mrtrix3 software, using a directional distribution function to track participants' main white matter fiber bundles. Demographic and clinical characteristics were recorded. Quantitative gait and clinical scales were used to assess the status of medication ON and OFF in PD patients.

Results: The axial kurtosis (AK), mean kurtosis (MK), and radial kurtosis (RK) of five specific white matter fiber tracts, the bilateral corticospinal tract, left superior longitudinal fasciculus, left anterior thalamic radiation, forceps minor, and forceps major were significantly higher in PD patients compared to HCs. Additionally, the MK values were negatively correlated with Timed Up and Go Test (TUG) scores in both the ON and OFF in PD patients. Within the PD group, higher AK, MK, and RK values, whether the patients were ON or OFF, were associated with better gait performance (i.e., higher velocity and stride length).

Conclusions: PD exhibits characteristic regional patterns of white matter microstructural degradation. Correlations between objective gait parameters and DKI values suggest that dopamine-responsive gait function depends on preserved white matter microstructure. DKI-based Tract-Based Spatial Statistics (TBSS) analysis may serve as a tool for evaluating PD-related motor impairments (e.g., gait impairment) and could yield potential neuroimaging biomarkers.

Keywords: Parkinson's disease; Gait impairment; ON/OFF state; Diffusion kurtosis imaging; White matter; Quantitative gait

Introduction

Parkinson's disease (PD) is a progressive neurodegenerative disorder that is associated with a variety of movement-related symptoms, including bradykinesia, myotonia, resting tremors, and postural and gait disturbances.[1] Gait impairment is a major symptom that drives declines in quality of life among PD patients. It also increases the risk of falls, fractures, and even death.[2]

PD-associated motor symptoms can be traced to the disease's underlying pathology, including injuries to the dopaminergic projections between the substantia nigra pars compacta and the basal ganglia (caudate nucleus and putamen of the striatum), as well as the concomitant appearance of alpha-synaptic protein-immunoreactive inclusions in the cytoplasm of the neurons (Lewy bodies) and of the neuronal processes of the Lewy neurons.[3,4] In pathophysiology, gait impairments are already evident when 80% of the dopaminergic neurons in the patient's striatum have been lost.[5,6] Given the intricacy of the systems that regulate normal gait, the neural mechanisms underlying gait impairment in PD remain incompletely understood.[7–10] In normal individuals, gait orchestration involves the integration of cognitive planning, initiation, and movement execution in concert with cognitive stimuli, emotional stimuli, and sensory stimuli from the external environment.[11] This process involves multiple nerve fiber bundles in the brain. Consequently, the underlying neurodegeneration in PD patients may affect the functioning

Access this article online

Quick Response Code:

Website: www.cmj.org

DOI: 10.1097/CM9.0000000000003486

Xuan Wei and Shiya Wang contributed equally to this work.

Correspondence to: Houzhen Tuo, Department of Neurology, Beijing Friendship Hospital, Capital Medical University, No. 95, Yong An Road, Xicheng District, Beijing 100050, China
E-Mail: tuohzh@sina.cn;
Zhenchang Wang, Department of Radiology, Beijing Friendship Hospital, Capital Medical University, No. 95, Yong An Road, Xicheng District, Beijing 100050, China
E-Mail: cjr.wzhch@vip.163.com

Chinese Medical Journal 2025;138(9)
Received: 05-08-2024; **Online:** 27-02-2025 **Edited by:** Ting Gao

of nerve fiber bundles involved in gait control systems, which then likely contributes to the development of gait impairment.

Gait impairment can occur in the early stage of PD or even in the preclinical stage, and as the disease progresses, the difficulty of treating it—whether with pharmacotherapy, physiotherapy, speech therapy, or even psychotherapy—increases accordingly.[12,13] Although the degeneration of dopaminergic neurons underlies disease progression in PD, timely disease identification and intervention may help protract symptom advancement. Recent work has identified several novel biomarkers, including cerebrospinal fluid and serum markers, which can be used for the early prediction of PD.[14] However, there is still a need to explore the intracerebral mechanisms associated with gait impairment in PD from multiple perspectives in order to improve treatment.

Neuroimaging is one such perspective that remains relatively underexplored in PD gait impairment research. Diffusion kurtosis imaging (DKI) represents a magnetic resonance imaging (MRI) sequence that primarily captures the non-Gaussian dispersion of water molecules in biological tissues.[15] Through the meticulous quantification of water molecule diffusion characteristics, DKI accurately reflects the information of microstructural transformations in neural tissues.[15] Its unique merit lies in the analysis of nerve fiber tissue integrity, which also facilitates the detection of minute microstructural alterations within the nervous system.[16] Of particular significance is its capability to monitor and evaluate nerve fiber bundle damage. By surveying the directional-specific kurtosis, DKI reflects the complexity of neural tissue in normal, developmental, and pathological states. Notably, DKI provides three kurtosis parameters along distinct orientations: axial kurtosis (AK), mean kurtosis (MK), and radial kurtosis (RK).[17] Previous work has suggested that decreases in RK are associated with demyelination, that changes in AK reflect axonal degeneration,[15,18] and that increases MK may indicate injury-associated microglial proliferation and increased axonal bead granulation.[19] This method can provide quantitative neurological information, which can further help us understand the mechanism of gait impairment in PD and provide a more accurate method for its early diagnosis and treatment.

Given that PD is associated with white matter changes, we hypothesized that there may be a correlation between altered diffusion kurtosis of certain cortical white matter tracts and gait impairment in the "ON state" or "OFF state" of PD patients. Previous research has rarely combined objective gait parameters and DKI to assess PD. Thus, in the present study, we examined diffusion kurtosis alterations of white matter fiber bundles in healthy control (HC) and PD patients. Based on the computerized gait blanket, we also determined the correlation between objective gait parameters and DKI indexes. This study aims to improve understanding of the pathologic changes underlying gait impairment in PD, contributing to early disease detection and treatment.

Methods

Participants

Two datasets were included in this study. All participants in each dataset were recruited between 2019 and 2020 at the Movement Disorders Program at the Beijing Friendship Hospital Capital Medical University. The PD cohort (dataset 1) consisted of 24 participants, all of whom met the UK Parkinson's Disease Society Brain Bank criteria.[20] The patients were between the ages of 40 years and 85 years and had no history of brain-affecting surgery, trauma, or addiction, and had no other neuropsychiatric diseases. The HC cohort (dataset 2) consisted of 29 healthy subjects aged between 40 years and 85 years. These participants exhibited good motor and cognitive functions and had no history of neurologic or psychiatric disorders, neurosurgery, trauma, or addiction. All participants signed informed consent forms before being included in the study. All experimental procedures and tests followed the guidelines of the Ethics Committees of Beijing Friendship Hospital, Capital Medical University (No. 2019-P2-283-02). The sample size was calculated using the Power Analysis and Sample Size Software 2021 (PASS, NCSS, LLC, Kaysville, Utah, USA, ncss.com/software/pass) and the details are shown in Supplementary Materials, http://links.lww.com/CM9/C312.

Clinical assessments

PD patients with gait impairments were identified based on their medical history and thorough assessment using the International Parkinson and Movement Disorder Society-Unified Parkinson's Disease Rating Scale (MDS-UPDRS) part-II (items 2.12 or 2.13) and part-III (items 3.10 or 3.11), with a minimum score of 1. The 29 PD patients were studied in two conditions, the "OFF state" (PD-OFF) and "ON state" (PD-ON). The "OFF state" required patients withdraw any anti-parkinsonian drugs for a minimum of 12 h prior to the experimental procedures.[21] The "ON state" referred to experiments that were conducted exactly 1 h after patients received a super-ON dose of levodopa (125% of their equivalent morning levodopa dose).[22] Motor function was assessed for each patient on the same day, using the full MDS-UPDRS, Berg Balance Scale (BBS), New Freezing of Gait Questionnaire (NFOGQ), Timed Up and Go Test (TUG), and with objective gait parameters, in both the "OFF state" (performed first) and "ON state" (performed later) experiments. Objective gait parameters were assessed using a 20-foot-long computerized Zeno Walkway Gait Analysis System (Proto Kinetics, Havertown, PA, USA) at a self-selected pace (SSP) and a fast pace (FP). Non-motor scales include the Parkinson's Disease Questionnaire-39 items (PDQ-39), Mini-Mental State Examination (MMSE), Beck Depression Inventory (BDI) score, Beck Anxiety Inventory (BAI) score, and Modified Apathy Evaluation Scale (MAES). Of note, for PD patients, MRI scanning and non-motor assessments (PDQ-39, MMSE, BDI, BAI, MAES) were only performed in the "OFF state".

MRI data acquisition and preprocessing

Diffusion-weighted (DW) images were acquired on a 3.0T MRI system (Prisma, Siemens, Erlangen, Germany) with a 64-channel phase-array head coil. The major acquisition parameters included: field-of-view (FOV) = 209 mm × 209 mm, matrix size = 116 × 116, slices = 84 (with no gap), voxel size = 1.8 mm × 1.8 mm × 1.8 mm, repetition time (TR) = 3000 ms, echo time (TE) = 81 ms, and flip angle = 90°.

For each subject, two-shell high angular resolution diffusion imaging (HARDI) data were acquired, including 1 non-DW image (b = 0 s/mm^2, B0) with phase-encoding in the anterior-posterior (AP) direction, 10 non-DW images (b = 0 s/mm^2) with phase-encoding in the posterior-anterior (PA) direction, 64 DW images from 64 non-collinear gradient directions with a b-value of 1000 s/mm^2 and phase-encoding in the PA direction, and 64 DW images from 64 non-collinear gradient directions with a b-value of 2000 and phase-encoding in the PA direction.

Three-Dimensional (3D) T1-weighted image for each participant was obtained using a magnetization prepared rapid gradient echo (MPRAGE) sequence. The imaging parameters for 3D T1-weighted images included: FOV = 224 mm × 256 mm, matrix size = 448 × 512, 192 sagittal slices, voxel size = 0.5 mm × 0.5 mm × 1 mm, TR = 2530 ms, TE = 2.98 ms, and flip angle = 7°.

MRI data preprocessing and DKI processing

Diffusion-weighted imaging (DWI) preprocessing was performed with an optimized pipeline introduced by Maximov *et al*[23]. First, DWI data underwent noise correction and Gibbs ringing correction using the Marchenko-Pastur principle component analysis (MP-PCA)[24] and the local subvoxel-shifts method proposed by Kellner *et al*[25] separately with Mrtrix3 (https://www.mrtrix.org).[26] Next, non-DW images with opposite phase encoding directions, AP directions, and PA directions were used to correct the echo-planar imaging geometric distortion with top-up function[27,28] offered in FMRIB's Software Library (FSL) 6.0.3 (https://fsl.fmrib.ox.ac.uk/fsl/docs/#/diffusion/topup/index).[29] Distortions appearing due to eddy currents, head motion, and susceptibility-originated artefacts were corrected by top-up and eddy[30] together in FSL 6.0.3. The B1 field inhomogeneity corrections for DWI data were performed using dwibiascorrect in Mrtrix3.[26] Finally, the 11 preprocessed non-DW images were averaged to generate the mean B0 image for the following processes. Consequently, the preprocessed DWI data included one B0 image, 64 DWI images with a b-value of 1000 s/mm^2, and 64 DWI images with a b-value of 2000 s/mm^2. All the DWI images (b = 0 s/mm^2, 1000 s/mm^2, 2000 s/mm^2) were used to calculate DKI metrics, including AK, MK, and RK, with the Diffusional Kurtosis Estimator (https://www.nitrc.org/projects/dke/). Only images with b = 0 s/mm^2 and 1000 s/mm^2 were used to calculate DTI metrics, including fractional anisotropy (FA) maps, with the dtifit function in FSL.[29] The 3D T1-weighted images were segmented using the CAT12 (Computational Anatomy Toolbox for Statistical Parametric Mapping) (http://www.neuro.uni-jena.de/cat/index.html) to generate brain images in T1 space (brain_T1).

Statistical analysis

Statistical analysis of demographic and clinical information was performed using SPSS version 25.0 (SPSS, Inc., Chicago, IL, USA). Statistical significance was set at P <0.05 (two-tailed). Tests of normality revealed that not all clinical and objective gait-measurement data met the assumption of normality.

Demographic and clinical characteristics of PD and HC individuals were described as number with percentages (%) for categorical variables and as the median with interquartile ranges (IQRs) for continuous variables. Categorical variables were analyzed with chi-squared (χ^2) tests and continuous variables with Student's t-tests or Wilcoxon rank-sum tests. The disease-relevant DKI measures and clinical scales (MDS-UPDRS-III scores, TUG test scores, and BBS scores) were assessed by calculating Pearson's or Spearman's rank correlations, as appropriate.

The Wilcoxon rank-sum test was used to compare gait parameters between PD patients and HCs. For PD patients, changes in the objective gait parameters between the "ON" and "OFF" states were analyzed using Wilcoxon Signed Ranks Test. Correlations between the DKI indicators and gait parameters were analyzed using Pearson's or Spearman's rank correlations, as appropriate.

The Tract-Based Spatial Statistics (TBSS)[31] from FSL was used to investigate whole brain white matter anomalies in the PD cohort. First, FA images were used to generate the mean FA skeleton following the steps of TBSS. Next, AK, MK, and RK data were projected onto the original mean FA skeleton to generate 4 Dimensional projection data using tbss_non_FA in FSL. Finally, voxel-wise between-group statistics on the skeletonized DKI metrics was carried out using the randomize tool in FSL, with age and sex as covariates (50,000 permutations, corrected for multiple comparisons with Threshold-Free Cluster Enhancement[32]) (P <0.05).

Results

Participant demographics and behavioral measures

Demographic and clinical data are shown in Table 1 and Table 2. No significant differences in age, sex, education, MMSE scores, or MAES scores were found between the PD and HC groups (all P >0.05). BAI and BDI scores were significantly higher in the PD group compared to the HC group [Table 1]. BBS scores were significantly lower and TUG values were significantly higher in the PD group compared to the HC group [Table 2]. Compared with the HC group, the PD group had lower gait velocity and step length [Table 2]. Finally, in the PD group, ON status reduced the TUG time, MDS-UPDRS-III scores (P <0.01), and MDS-UPDRS total scores (P <0.05) when compared with OFF status [Table 2].

Table 1: Demographic and clinical characteristics (Non-motion) of the control and PD participants in the PD diffusion kurtosis study.

Variables	PD participants ($n = 24$)	Control participants ($n = 29$)	Statistical values	*P*-value
Age (years)	68.0 (63.3–70.0)	64.0 (51.5–70.0)	–1.522*	0.128
Male sex	10 (41.7)	14 (48.3)	0.232†	0.630
Education (>9 years)	12 (50.0)	15 (51.7)	0.016†	0.901
Disease duration (months)	52.0 (27.3–81.8)	–	–	–
MMSE	29.0 (29.8–28.0)	29.0 (30.0–27.0)	–0.598*	0.550
MASE	10.5 (4.3–17.0)	7.0 (5.0–13.0)	–1.163*	0.245
BAI	26.0 (24.0–29.8)	24.0 (22.0–25.5)	–3.055*	0.002
BDI	6.0 (4.0–9.0)	3.0 (1.0–4.5)	–3.349*	<0.001
LEDD (mg)	550.0 (318.8–743.8)	–	–	–
NFOGQ	10.0 (41.7%)	–	–	–
PDQ-39	20.5 (11.5–33.3)	–	–	–

Data are shown as *n* (%) or mean (interquartile range). *Z score between the PD and control group. †χ^2 values between the PD and control group. PD: Parkinson's disease; MMSE: Mini-Mental State Examination; MASE: Modified Apathy Estimate Scale; BAI: Beck Anxiety Inventory; BDI: Beck Depression Inventory; LEDD: Levodopa equivalent daily dose (mg); NFOGQ: New Freezing of Gait Questionnaire; PDQ-39: Parkinson's Disease Questionnaire-39 items; –: Not applicable. The same set of clinical data from the control was used to analyze against the PD group.

Table 2: Motor characteristics of the control and PD participants in the PD diffusion kurtosis study.

	PD				Control				
						Statistical values		*P*-value	
Variables	"ON state"	"OFF state"	Statistical values	*P*-value	Participants ($n = 29$)	"ON state"	"OFF state"	"ON state"	"OFF state"
MDS-UPDRS-III	16.0 (12.5–23.8)	29.5 (20.0–36.8)	–4.393*	<0.001	–	–		–	
MDS-UPDRS Total	39.5 (25.0–46.8)	48.0 (34.3–62.5)	–2.135†	0.033	–	–		–	
TUG	8.8 (8.2–10.2)	10.5 (9.0–12.2)	–2.031†	0.042	8.1 (7.3–8.6)	–3.091‡	–4.709§	0.002	<0.001
BBS	52.0 (44.3–54.0)	49.5 (39.3–52.8)	–1.674†	0.094	56.0 (54.0–56.0)	–4.459‡	–5.307§	<0.001	<0.001
Velocity SSP (cm/s)	105.2 (86.5–118.9)	104.4 (79.1–113.5)	–0.577†	0.564	117.0 (106.9–133.0)	–2.698‡	–3.163§	0.007	0.002
Cadence SSP (step/min)	114.3 (105.5–119.1)	113.4 (107.7–120.5)	–0.577†	0.564	112.5 (106.6–121.4)	–0.059‡	–0.125§	0.555	0.900
Stride time SSP (s)	1.0 (1.0–1.1)	1.1 (1.0–1.1)	–0.320†	0.749	1.1 (1.0–1.1)	–0.143‡	–0.545§	0.886	0.586
Stride length SSP (cm)	110.9 (96.3–124.4)	106.1 (88.7–120.4)	–0.660†	0.509	127.8 (114.8–136.0)	–2.984‡	–4.420‖	0.003	<0.001
Velocity FP (cm/s)	126.9 (109.1–142.8)	123.7 (103.0–137.7)	0.777*	0.441	147.1 (139.6–168.4)	–3.677¶	–4.527‖	<0.001	<0.001
Cadence FP (step/min)	123.4 (114.6–132.2)	125.8 (114.9–132.3)	–0.309†	0.757	129.6 (119.7–136.4)	–1.805‡	–1.519§	0.071	0.129
Stride time FP (s)	1.0 (0.9–1.0)	1.0 (0.9–1.0)	–0.278†	0.781	0.9 (0.9–1.0)	–1.626‡	–1.358§	0.104	0.174
Stride length FP (cm)	122.7 (108.7–138.5)	120.4 (101.4–129.2)	1.024*	0.311	138.3 (127.9–152.6)	–3.143¶	–4.154‖	0.003	<0.001

Data are shown as mean (interquartile range). **t* values between "ON state" and "OFF state" data in 24 patients with PD. †*Z* score between "ON state" and "OFF state" data in 24 patients with PD. ‡*Z* score between patients with PD in "ON state" and control group. §*Z* score between patients with PD in "OFF state" and control group. ‖*t* values between patients with PD in "OFF state" and control group. ¶*t* values between patients with PD in "ON state" and control group. PD: Parkinson's disease; MDS-UPDRS: International Parkinson and Movement Disorder Society Unified Parkinson's Disease Rating Scale; MDS-UPDRS-III: MDS-UPDRS motor score; TUG: Timed Up and Go Test; BBS: Berg Balance Scale; SSP: Self-selected pace; FP: Fast pace; –: Not applicable. For control, there is no ON or OFF state. The same set of clinical data from the control was used to analyze against the PD group.

Tract-based spatial statistics data

There were significant between-group differences in broad fibers (P <0.05, corrected by Threshold-Free Cluster Enhancement; Figure 1). The white matter tracts with significant between-group AK differences included the corticospinal tract, superior longitudinal fasciculus, cingulum, anterior thalamic radiation, and forceps minor. The white matter tracts with significant between-group MK differences included the forceps minor, forceps major, anterior thalamic radiation, corticospinal tract, and left inferior fronto-occipital fasciculus. The white matter tracts with significant between-group RK

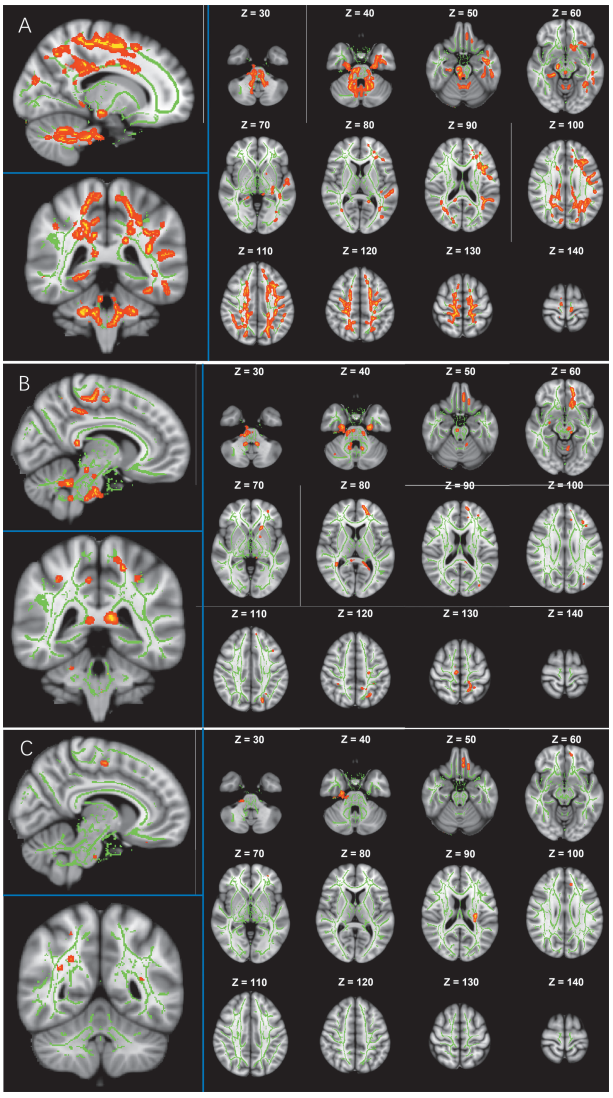

Figure 1: Voxel-wise TBSS analysis comparing PD patients and HCs for AK (A), MK (B), and RK (C) metrics. Significant voxel-wise group differences (P <0.05, corrected using Threshold-Free Cluster Enhancement) are shown in red, overlaid on axial sections of the white-matter skeleton (green). The left side of each image corresponds to the right brain hemisphere. Z-coordinates indicate slice positions in MNI space. (A) AK: Significant differences in the corticospinal tract, superior longitudinal fasciculus, cingulum, anterior thalamic radiation, and forceps minor. (B) MK: Significant differences in the forceps minor, forceps major, anterior thalamic radiation, corticospinal tract, and left inferior fronto-occipital fasciculus. (C) RK: Significant differences in the left corticospinal tract and forceps minor. AK: Axial kurtosis; HCs: Healthy controls; AK: Axial kurtosis; PD: Parkinson's disease; RK: Radial kurtosis; TBSS: Tract-Based Spatial Statistics.

differences included the left corticospinal tract and forceps minor.

As shown in Figure 2, the AK, MK, and RK values of specific white matter fiber bundles were significantly increased in PD patients compared to their HC counterparts, and these differences remained significant even after adjusting for age and sex (P <0.05).

Correlation analysis

MK values in the forceps minor were negatively correlated with both TUG-ON (TUG scores in "ON state") and TUG-OFF (TUG scores in "OFF state") (r = –0.410, P = 0.047 and r = –0.450, P = 0.028; Supplementary Figure 2, http://links.lww.com/CM9/C312). There were no significant correlations between any DKI model metrics and BBS, BDI, BAI, MMSE, MAES, PDQ-39, MDS-UPDRS, or NFOGQ.

Table 3 displays the Pearson's or Spearman's correlation coefficients for several DKI measures that were strongly correlated with objective gait parameters in PD patients. Focusing on velocity, AK values were positively correlated with both SSP and FP under the ON and OFF states (ON, SSP: r = 0.566, P = 0.004; OFF, SSP: r = 0.493, P = 0.014; ON, FP: r = 0.485, P = 0.016; OFF, FP: r = 0.471, P = 0.020; Table 3). Furthermore, at SSP, a higher AK value was significantly correlated with longer stride times in the ON states in PD patients (r = 0.469, P = 0.021; Table 3). MK values were positively correlated with velocity and stride length in almost all states (velocity, ON, SSP: r = 0.656, P = 0.001; velocity, OFF, SSP: r = 0.564, P = 0.004; velocity, ON, FP: r = 0.560, P = 0.004; velocity, OFF, FP: r = 0.523, P = 0.009; stride length, ON, SSP: r = 0.550, P = 0.005; stride length, OFF, SSP: r = 0.429, P = 0.037; stride length, ON, FP: r = 0.463, P = 0.023; Table 3). Finally, in the "ON state", higher RK values during SSP were significantly associated with greater velocity and stride length (r = 0.466, P = 0.022 and r = 0.435, P = 0.034; Table 3).

Discussion

In the present study, we utilized DKI techniques to investigate white matter changes and their correlations with gait parameters in PD patients. First, we examined whole-brain white matter differences between a group of PD patients and a group of HC participants. Based on those findings, we analyzed the correlations between DKI index scores and clinical scales, as well as between DKI scores and objective gait parameters. The main findings were as follows: (1) significant differences between HC and PD patients were identified in the whole brain white matter; (2) specific white matter changes were correlated with TUG-ON and TUG-OFF in PD patients; and (3) specific white matter changes were correlated with objective gait parameters in PD patients.

DKI analysis demonstrates microstructural characteristics of the brain

DKI, a non-Gaussian water molecular dispersion technique[17,33] for describing complex tissues, can be used to detect microstructural changes in cortical white matter[34] based on the following parameters[15]: AK, MK, and RK.

MK represents the average of upward diffusion kurtosis of all spatial parties, independent of the spatial orientation of organizational structure, and can be used in the analysis of gray and white matter.[35–37] MK values are also related to structural complexity.[38] The higher the structural complexity, the more the dispersion of the water molecules in the structure that do not conform to Gaussian distributions, and the higher the MK value.[39] RK refers to the average kurtosis value in the main dispersion orthogonal direction and mainly describes the dispersion kurtosis

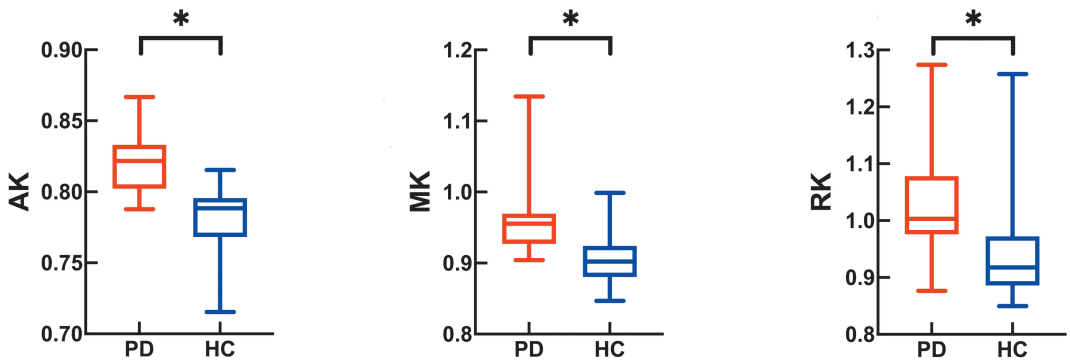

Figure 2: Compared with the PD group, the DKI metrics (AK, MK, and RK) were significantly decreased across multiple white matter areas in the HC group. *P <0.01. AK: Axial kurtosis; DKI: Diffusion kurtosis imaging; HC: Healthy control; MK: Mean kurtosis; PD: Parkinson's disease; RK: Radial kurtosis.

Table 3: Correlation between DKI values and different gait measures in the PD diffusion kurtosis study.

	AK Person correlation		MK Spearman correlation		RK Spearman correlation	
Gait measures	***r***	***P*-value**	***r***	***P*-value**	***r***	***P*-value**
SSP						
ON						
Velocity (cm/s)	0.566	0.004	0.656	0.001	0.466	0.022
Stride length (cm)	0.469	0.021	0.550	0.005	0.435	0.034
OFF						
Velocity (cm/s)	0.493	0.014	0.564	0.004	0.367	0.078
Stride length (cm)	0.395	0.056	0.429	0.037	0.246	0.246
FP						
ON						
Velocity (cm/s)	0.485	0.016	0.560	0.004	0.324	0.122
Stride length (cm)	0.393	0.057	0.463	0.023	0.404	0.050
OFF						
Velocity (cm/s)	0.471	0.020	0.523	0.009	0.361	0.083
Stride length (cm)	0.400	0.053	0.372	0.073	0.276	0.192

AK: Axial kurtosis; DKI: Diffusion kurtosis imaging; FP: Fast pace; MK: Mean kurtosis; OFF: In medication "OFF state"; ON: In medication "ON state"; RK: Radial kurtosis; SSP: Self-selected pace.

value perpendicular to the fiber direction.[40] The more restricted the dispersion of non-normal water molecules in the direction of the vertical fiber bundle, the higher the RK value.[39] Finally, AK values reflect the dispersion in the direction parallel to the white matter bundle.[40] Since AK values are generally significantly lower than the RK values, the sensitivity for detecting AK changes is higher when the dispersion movement of water molecules in the direction of the white matter tract changes.[40]

Previous DKI research has demonstrated microstructural changes in PD patients when they are compared with HC. Most studies have shown that PD patients have higher MK values than HC,[39,41–44] but the findings related to AK and RK values in PD have not been consistent.[43] Some studies have found increases in AK or RK in specific cortical areas in PD patients,[43,45,46] and others have found opposite trends.[47,48] However, most studies[41,49] have not found any AK or RK differences between PD patients and HC. Therefore, these changes need to be further studied.

When we compared TBSS-based white matter changes between the PD cohort with the gait impairment and the HC cohort, we did find that PD patients had higher DKI values (including AK, MK, and RK values) compared to HC. These changes may be related to the increased structural complexity of the white matter, which could be driven by several neurobiological causes: (1) the formation of Lewy bodies increases structural complexity, thus increasing DKI values;[50] (2) the absence of neurons in the fiber tracts leads to secondary microglial cell aggregation and damage repair, increasing the structural complexity and thus DKI values;[41,51,52] (3) oxidative stress and chronic inflammation lead to restricted diffusion of water molecules, resulting in elevated DKI values;[53,54] and (4) increased iron content in neuronal cells, which reduces the signal-to-noise ratio and leads to elevated DKI values.[55]

White matter degeneration is associated with gait impairment

We also found that gait impairment could be related to microstructural white matter changes in PD. Specifically, alterations in the bilateral corticospinal tract, left superior longitudinal fasciculus, left anterior thalamic radiation,

forceps minor, and forceps major were related to gait impairment in our PD cohort.

Previous studies have indicated that these five white matter fiber bundles do affect gait. Wei *et al*[56] found significant differences in neurite orientation dispersion and density imaging (NODDI) indices in the anterior thalamic radiation, corticospinal tract, superior longitudinal fasciculus, forceps major, cingulum, and inferior longitudinal fasciculus in PD patients compared to HC. Vercruysse *et al*[57] identified that microstructural changes associated with PD can spread through several subcortical white matter layers, including the intra-hemispheric cortico-cortical association fibers of the superior longitudinal fasciculus, the motor-related corticofugal tract, and the thalamic radiation. Verlinden *et al*[58] reported significant microstructural changes in the thalamic radiations, association tracts, and forceps major and that these changes were strongly associated with gait impairment in PD. Based on diffusion tensor imaging, Marumoto *et al*[59] observed significant changes in the anterior thalamic radiation and forceps minor. Based on the consistency of these findings with our own, we can infer that microstructure alteration in cortical white matter tracts might be closely related to gait impairment in PD. The vulnerability of white matter fiber bundles is anatomically selective and may be related to the functional anatomy of gait control. Thus, white matter changes in the bilateral corticospinal tract, left superior longitudinal fasciculus, left anterior thalamic radiation, forceps minor, and forceps major may underlie gait impairment in PD.

It is also important to note that, although we found significant associations between numerous white matter tracts and gait parameters, the tract that was most strongly correlated with these parameters was the left superior longitudinal fasciculus.[60] Figure 1 shows that the left superior longitudinal fasciculus also had the highest relative weight. This finding suggests that the white matter with the most microstructural changes played a disproportionate role in determining gait changes.

DKI values correlate with clinical indicators in PD

PD patients' motor functioning was assessed using clinical scales and objective gait parameters. To further clarify which specific clinical markers of gait were associated with alterations in white matter, we correlated clinical indicators and objective gait parameters with DKI values.

We found that as MK values increased, TUG scores also increased (irrespective of PD ON or OFF state), suggesting a correlation between the structural complexity of the white matter tissues and the severity of motor symptoms in PD.[56] In terms of gait parameters, PD patients had significantly lower stride velocity and length compared to HC. Therefore, we only chose these significant measures (velocity and stride length) to correlate with DKI values. We found a positive relationship between these measures and a specific DKI index: higher AK values in the left superior longitudinal fasciculus correlated with higher stride velocities, suggesting that microstructural disruption in this region may also underlie gait impairment in PD.[57] There were also more correlations between various DKI parameters and gait parameters among PD patients in the "ON state", suggesting levodopa could potentially be attributed to its partial activation of these white matters, consequently modifying their network connectivity and influencing the microstructure of these white matters.[56,61] "OFF state" measurements reflect the PD inherent condition, unaffected by dopaminergic interventions.[62] The elevated DKI values, indicative of a superior degree of the white matter complexity, correlate with improved gait parameters in the "OFF state", aligning coherently with the hypothesis that the gait parameters responsive to dopamine necessitate a substantially preserved white matter integrity.

Thus, we speculate that AK, MK, and RK values may be related to the formation of Lewy bodies, the aggregation of microglia, and/or the repair of neurons rather than neuronal loss because they reflect increases in microstructural complexity (as would be seen in these aggregative/repair processes), not decrease (as would be seen in neuronal loss). In other words, although neurons are lost, the aggregation of other repair cells and inflammatory factors results in relatively timely repair and replacement, leading to corresponding increases in velocity and stride length. Therefore, correlations were found between gait measures and DKI indices, suggesting that microstructural alterations in these white matters may be the underlying cause of gait impairment in PD.[56] Among DKI values, MK values were the most strongly correlated with objective gait parameters, suggesting that individual DKI values could be used as independent parameters of gait impairment in PD patients. We also identified relatively more correlations between various DKI parameters and gait parameters among PD patients in the "ON state", suggesting that levodopa may partially activate, and thus preferentially act on these white matter areas.[56,62]

In recent years, many efforts have been made to examine brain microstructural changes and their effects in patients with PD. Our study applied neuroimaging to offer new insights into microstructural alterations and the associated changes in objective gait parameters in this population. Tracking microstructural changes in PD compared to HC will help us better understand the microstructural alterations underlying the pathogenesis of PD, and will aid in the development of new approaches to monitor and treat PD. However, because we hope to establish a reliable imaging portfolio for gait changes in the early stages of PD, it is important to determine whether a combination of DKI metrics and gait parameters can detect microstructural changes in the brain in this early disease state. In future studies, we plan to combine other structural and functional MRI techniques to enhance our understanding of PD-associated brain microstructural changes and to establish a more reliable imaging approach to identifying gait impairment in neurodegenerative disease.

The main limitation of this study was that the correlation coefficients between our objective gait parameters and DKI values were not high. This may be because DKI values were not the only factors affecting gait—it could also be impacted by age, cognition, and the course of

disease, for example. Nonetheless, our study still provided novel imaging insights into the mechanism underlying gait impairment in PD patients. Another limitation was that the number of participants in each group was relatively small.

In summary, our study identified an important and specific pattern of white matter changes—namely, we found elevated DKI values in specific white matter fiber bundles of PD participants. We also found correlations between the objective gait parameters and white matter DKI values among patients with gait impairment, suggesting that brain microstructure changes in specific white matter tracts may affect gait in PD. These correlations in the "ON state" or "OFF state" of PD patients indicate that dopamine-responsive gait parameters rely on a preserved white matter integrity. Our findings may ultimately provide imaging markers for the early identification of and intervention for gait impairment in PD patients.

Acknowledgement

We sincerely appreciate the assistance provided by the Department of Radiology, Beijing Friendship Hospital, Capital Medical University, in the collection of the imaging data. We extend our gratitude to Dr. Sangma Xie for their valuable support in coordinating and performing the data preprocessing tasks for this project.

Funding

This work was supported by grants from the National Natural Science Foundation of China (Nos. 82202097, 82371254 and 82071257); Beijing Hospitals Authority' Youth Programme (No. QML20230113); Training Fund for Open Projects at Clinical Institutes and Departments of Capital Medical University (No. CCMU2022Z-KYXY010); Beijing Scholars Program (No. [2015] 160); Tongzhou District Health Development Program (No. KJ2024CX023); and Beijing Municipal Bureau of Economy and Information Technology (No. JX2023YJ021).

Conflicts of interest

None.

References

1. Kalia LV, Lang AE. Parkinson's disease. Lancet 2015;386:896–912. doi: 10.1016/s0140-6736(14)61393-3.
2. López IC, Ruiz PJ, Del Pozo SV, Bernardos VS. Motor complications in Parkinson's disease: Ten year follow-up study. Mov Disord 2010;25:2735–2739. doi: 10.1002/mds.23219.
3. Przedborski S. The two-century journey of Parkinson disease research. Nat Rev Neurosci 2017;18:251–259. doi: 10.1038/nrn.2017.25.
4. Covell DJ, Robinson JL, Akhtar RS, Grossman M, Weintraub D, Bucklin HM, *et al*. Novel conformation-selective alpha-synuclein antibodies raised against different in vitro fibril forms show distinct patterns of Lewy pathology in Parkinson's disease. Neuropathol Appl Neurobiol 2017;43:604–620. doi: 10.1111/nan.12402.
5. Obeso JA, Rodríguez-Oroz MC, Rodríguez M, Lanciego JL, Artieda J, Gonzalo N, *et al*. Pathophysiology of the basal ganglia in Parkinson's disease. Trends Neurosci 2000;23(Suppl):S8–S19. doi: 10.1016/s1471-1931(00)00028-8.
6. Tagliaferro P, Burke RE. Retrograde Axonal Degeneration in Parkinson Disease. J Parkinsons Dis. 2016;6:1–15. doi: 10.3233/JPD-150769.
7. Ouchi Y, Kanno T, Okada H, Yoshikawa E, Futatsubashi M, Nobezawa S, *et al*. Changes in dopamine availability in the nigrostriatal and mesocortical dopaminergic systems by gait in Parkinson's disease. Brain 2001;124:784–792. doi: 10.1093/brain/124.4.784.
8. Obeso JA, Rodríguez-Oroz MC, Benitez-Temino B, Blesa FJ, Guridi J, Marin C, *et al*. Functional organization of the basal ganglia: Therapeutic implications for Parkinson's disease. Mov Disord 2008;23(Suppl 3):S548–S559. doi: 10.1002/mds.22062.
9. Nutt JG, Bloem BR, Giladi N, Hallett M, Horak FB, Nieuwboer A. Freezing of gait: Moving forward on a mysterious clinical phenomenon. Lancet Neurol 2011;10:734–744. doi: 10.1016/s1474-4422(11)70143-0.
10. Giladi N, Treves TA, Simon ES, Shabtai H, Orlov Y, Kandinov B, *et al*. Freezing of gait in patients with advanced Parkinson's disease. J Neural Transm (Vienna) 2001;108:53–61. doi: 10.1007/s007020170096.
11. Takakusaki K. Functional neuroanatomy for posture and gait control. J Mov Disord 2017;10:1–17. doi: 10.14802/jmd.16062.
12. Wu Z, Jiang X, Zhong M, Shen B, Zhu J, Pan Y, *et al*. Mild gait impairment and its potential diagnostic value in patients with early-stage Parkinson's disease. Behav Neurol 2021;2021:6696454. doi: 10.1155/2021/6696454.
13. Grajić M, Stanković I, Radovanović S, Kostić V. Gait in drug naïve patients with *de novo* Parkinson's disease–altered but symmetric. Neurol Res 2015;37:712–716. doi: 10.1179/1743132815y.0000000043.
14. Parnetti L, Gaetani L, Eusebi P, Paciotti S, Hansson O, El-Agnaf O, *et al*. CSF and blood biomarkers for Parkinson's disease. Lancet Neurol 2019;18:573–586. doi: 10.1016/s1474-4422(19)30024-9.
15. Arab A, Wojna-Pelczar A, Khairnar A, Szabó N, Ruda-Kucerova J. Principles of diffusion kurtosis imaging and its role in early diagnosis of neurodegenerative disorders. Brain Res Bull 2018;139:91–98. doi: 10.1016/j.brainresbull.2018.01.015.
16. Das SK, Wang JL, Bing L, Bhetuwal A, Yang HF. Regional values of diffusional kurtosis estimates in the healthy brain during normal aging. Clin Neuroradiol 2017;27:283–298. doi: 10.1007/s00062-015-0490-z.
17. Jensen JH, Helpern JA, Ramani A, Lu H, Kaczynski K. Diffusional kurtosis imaging: The quantification of non-Gaussian water diffusion by means of magnetic resonance imaging. Magn Reson Med 2005;53:1432–1440. doi: 10.1002/mrm.20508.
18. Cheung MM, Hui ES, Chan KC, Helpern JA, Qi L, Wu EX. Does diffusion kurtosis imaging lead to better neural tissue characterization? A rodent brain maturation study. Neuroimage 2009;45:386–392. doi: 10.1016/j.neuroimage.2008.12.018.
19. Weber RA, Hui ES, Jensen JH, Nie X, Falangola MF, Helpern JA, *et al*. Diffusional kurtosis and diffusion tensor imaging reveal different time-sensitive stroke-induced microstructural changes. Stroke 2015;46:545–550. doi: 10.1161/strokeaha.114.006782.
20. Hughes AJ, Daniel SE, Ben-Shlomo Y, Lees AJ. The accuracy of diagnosis of Parkinsonian syndromes in a specialist movement disorder service. Brain 2002;125:861–870. doi: 10.1093/brain/awf080.
21. Chen L, Bedard P, Hallett M, Horovitz SG. Dynamics of top-down control and motor networks in Parkinson's disease. Mov Disord 2021;36:916–926. doi: 10.1002/mds.28461.
22. Tomlinson CL, Stowe R, Patel S, Rick C, Gray R, Clarke CE. Systematic review of levodopa dose equivalency reporting in Parkinson's disease. Mov Disord 2010;25:2649–2653. doi: 10.1002/mds.23429.
23. Maximov II, Alnaes D, Westlye LT. Towards an optimised processing pipeline for diffusion magnetic resonance imaging data: Effects of artefact corrections on diffusion metrics and their age associations in UK Biobank. Hum Brain Mapp 2019;40:4146–4162. doi: 10.1002/hbm.24691.
24. Veraart J, Fieremans E, Novikov DS. Diffusion MRI noise mapping using random matrix theory. Magn Reson Med 2016;76:1582–1593. doi: 10.1002/mrm.26059.
25. Kellner E, Dhital B, Kiselev VG, Reisert M. Gibbs-ringing artifact removal based on local subvoxel-shifts. Magn Reson Med 2016;76:1574–1581. doi: 10.1002/mrm.26054.
26. Tournier JD, Smith R, Raffelt D, Tabbara R, Dhollander T, Pietsch M, *et al*. MRtrix3: A fast, flexible and open software framework for medical image processing and visualisation. Neuroimage 2019;202:116137. doi: 10.1016/j.neuroimage.2019.116137.

27. Andersson JL, Skare S, Ashburner J. How to correct susceptibility distortions in spin-echo echo-planar images: Application to diffusion tensor imaging. Neuroimage 2003;20:870–888. doi: 10.1016/s1053-8119(03)00336-7.
28. Smith SM, Jenkinson M, Woolrich MW, Beckmann CF, Behrens TE, Johansen-Berg H, *et al*. Advances in functional and structural MR image analysis and implementation as FSL. Neuroimage 2004;23(Suppl 1):S208–S219. doi: 10.1016/j.neuroimage.2004.07.051.
29. Jenkinson M, Beckmann CF, Behrens TE, Woolrich MW, Smith SM. FSL. Neuroimage 2012;62:782–790. doi: 10.1016/j.neuroimage.2011.09.015.
30. Andersson JLR, Sotiropoulos SN. An integrated approach to correction for off-resonance effects and subject movement in diffusion MR imaging. Neuroimage 2016;125:1063–1078. doi: 10.1016/j.neuroimage.2015.10.019.
31. Smith SM, Jenkinson M, Johansen-Berg H, Rueckert D, Nichols TE, Mackay CE, *et al*. Tract-based spatial statistics: Voxel-wise analysis of multi-subject diffusion data. Neuroimage 2006;31:1487–1505. doi: 10.1016/j.neuroimage.2006.02.024.
32. Winkler AM, Ridgway GR, Webster MA, Smith SM, Nichols TE. Permutation inference for the general linear model. Neuroimage 2014;92:381–397. doi: 10.1016/j.neuroimage.2014.01.060.
33. Jensen JH, Helpern JA. MRI quantification of non-Gaussian water diffusion by kurtosis analysis. NMR Biomed 2010;23:698–710. doi: 10.1002/nbm.1518.
34. Umesh Rudrapatna S, Wieloch T, Beirup K, Ruscher K, Mol W, Yanev P, *et al*. Can diffusion kurtosis imaging improve the sensitivity and specificity of detecting microstructural alterations in brain tissue chronically after experimental stroke? Comparisons with diffusion tensor imaging and histology. Neuroimage 2014;97:363–373. doi: 10.1016/j.neuroimage.2014.04.013.
35. Johnson NA, Jahng GH, Weiner MW, Miller BL, Chui HC, Jagust WJ, *et al*. Pattern of cerebral hypoperfusion in Alzheimer disease and mild cognitive impairment measured with arterial spin-labeling MR imaging: Initial experience. Radiology 2005;234:851–859. doi: 10.1148/radiol.2343040197.
36. Guglielmetti C, Veraart J, Roelant E, Mai Z, Daans J, Van Audekerke J, *et al*. Diffusion kurtosis imaging probes cortical alterations and white matter pathology following cuprizone induced demyelination and spontaneous remyelination. Neuroimage 2016;125:363–377. doi: 10.1016/j.neuroimage.2015.10.052.
37. Zhuo J, Xu S, Proctor JL, Mullins RJ, Simon JZ, Fiskum G, *et al*. Diffusion kurtosis as an *in vivo* imaging marker for reactive astrogliosis in traumatic brain injury. Neuroimage 2012;59:467–477. doi: 10.1016/j.neuroimage.2011.07.050.
38. Wang D, Guo ZH, Liu XH, Li YH, Wang H. Examination of hippocampal differences between Alzheimer disease, amnestic mild cognitive impairment and normal aging: Diffusion kurtosis. Curr Alzheimer Res 2015;12:80–87. doi: 10.2174/1567205012666141218142422.
39. Zhang G, Zhang Y, Zhang C, Wang Y, Ma G, Nie K, *et al*. Diffusion kurtosis imaging of substantia nigra is a sensitive method for early diagnosis and disease evaluation in Parkinson's disease. Parkinsons Dis 2015;2015:207624. doi: 10.1155/2015/207624.
40. Steven AJ, Zhuo J, Melhem ER. Diffusion kurtosis imaging: An emerging technique for evaluating the microstructural environment of the brain. AJR Am J Roentgenol 2014;202:W26–W33. doi: 10.2214/ajr.13.11365.
41. Wang JJ, Lin WY, Lu CS, Weng YH, Ng SH, Wang CH, *et al*. Parkinson disease: Diagnostic utility of diffusion kurtosis imaging. Radiology 2011;261:210–217. doi: 10.1148/radiol.11102277.
42. Sejnoha Minsterova A, Klobusiakova P, Pies A, Galaz Z, Mekyska J, Novakova L, *et al*. Patterns of diffusion kurtosis changes in Parkinson's disease subtypes. Parkinsonism Relat Disord 2020;81:96–102. doi: 10.1016/j.parkreldis.2020.10.032.
43. Yang L, Cheng Y, Sun Y, Xuan Y, Niu J, Guan J, *et al*. Combined application of quantitative susceptibility mapping and diffusion kurtosis imaging techniques to investigate the effect of iron deposition on microstructural changes in the brain in Parkinson,s disease. Front Aging Neurosci 2022;14:792778. doi: 10.3389/fnagi.2022.792778.
44. Welton T, Hartono S, Shih YC, Lee W, Chai PH, Chong SL, *et al*. Microstructure of brain nuclei in early Parkinson's disease: Longitudinal diffusion kurtosis imaging. J Parkinsons Dis 2023;13:233–242. doi: 10.3233/JPD-225095.
45. Khairnar A, Latta P, Drazanova E, Ruda-Kucerova J, Szabó N, Arab A, *et al*. Diffusion kurtosis imaging detects microstructural alterations in brain of α-synuclein overexpressing transgenic mouse model of Parkinson's disease: A pilot study. Neurotox Res 2015;28:281–289. doi: 10.1007/s12640-015-9537-9.
46. Bingbing G, Yujing Z, Yanwei M, Chunbo D, Weiwei W, Shiyun T, *et al*. Diffusion kurtosis imaging of microstructural changes in gray matter nucleus in Parkinson disease. Front Neurol 2020;11:252. doi: 10.3389/fneur.2020.00252.
47. Bai X, Zhou C, Guo T, Guan X, Wu J, Liu X, *et al*. Progressive microstructural alterations in subcortical nuclei in Parkinson's disease: A diffusion magnetic resonance imaging study. Parkinsonism Relat Disord 2021;88:82–89. doi: 10.1016/j.parkreldis.2021.06.003.
48. Takeshige-Amano H, Hatano T, Kamagata K, Andica C, Uchida W, Abe M, *et al*. White matter microstructures in Parkinson's disease with and without impulse control behaviors. Ann Clin Transl Neurol 2022;9:253–263. doi: 10.1002/acn3.51504.
49. Lench DH, Keith K, Wilson S, Padgett L, Benitez A, Ramakrishnan V, *et al*. Neurodegeneration of the globus pallidus internus as a neural correlate to dopa-response in freezing of gait. J Parkinsons Dis 2022;12:1241–1250. doi: 10.3233/jpd-213062.
50. Giannelli M, Toschi N, Passamonti L, Mascalchi M, Diciotti S, Tessa C. Diffusion kurtosis and diffusion-tensor MR imaging in Parkinson disease. Radiology 2012;265:645–646;authorrely646–647. doi: 10.1148/radiol.12121036.
51. Zhou Y, Zhu J, Lv Y, Song C, Ding J, Xiao M, *et al*. Kir6.2 deficiency promotes mesencephalic neural precursor cell differentiation via regulating miR-133b/GDNF in a Parkinson's disease mouse model. Mol Neurobiol 2018;55:8550–8562. doi: 10.1007/s12035-018-1005-0.
52. Imamura K, Hishikawa N, Sawada M, Nagatsu T, Yoshida M, Hashizume Y. Distribution of major histocompatibility complex class II-positive microglia and cytokine profile of Parkinson's disease brains. Acta Neuropathol 2003;106:518–526. doi: 10.1007/s00401-003-0766-2.
53. McGeer PL, McGeer EG. Inflammation and neurodegeneration in Parkinson's disease. Parkinsonism Relat Disord 2004;10(Suppl 1):S3–S7. doi: 10.1016/j.parkreldis.2004.01.005.
54. Block ML, Zecca L, Hong JS. Microglia-mediated neurotoxicity: Uncovering the molecular mechanisms. Nat Rev Neurosci 2007;8:57–69. doi: 10.1038/nrn2038.
55. Wang JY, Zhuang QQ, Zhu LB, Zhu H, Li T, Li R, *et al*. Meta-analysis of brain iron levels of Parkinson's disease patients determined by postmortem and MRI measurements. Sci Rep 2016;6:36669. doi: 10.1038/srep36669.
56. Wei X, Wang S, Zhang M, Yan Y, Wang Z, Wei W, *et al*. Gait impairment-related axonal degeneration in Parkinson's disease by neurite orientation dispersion and density imaging. NPJ Parkinsons Dis 2024;10:45. doi: 10.1038/s41531-024-00654-w.
57. Vercruysse S, Leunissen I, Vervoort G, Vandenberghe W, Swinnen S, Nieuwboer A. Microstructural changes in white matter associated with freezing of gait in Parkinson's disease. Mov Disord 2015;30:567–576. doi: 10.1002/mds.26130.
58. Verlinden VJ, de Groot M, Cremers LG, van der Geest JN, Hofman A, Niessen WJ, *et al*. Tract-specific white matter microstructure and gait in humans. Neurobiol Aging 2016;43:164–173. doi: 10.1016/j.neurobiolaging.2016.04.005.
59. Marumoto K, Koyama T, Hosomi M, Kodama N, Miyake H, Domen K. Diffusion tensor imaging in elderly patients with idiopathic normal pressure hydrocephalus or Parkinson's disease: Diagnosis of gait abnormalities. Fluids Barriers CNS 2012;9:20. doi: 10.1186/2045-8118-9-20.
60. Alzaid H, Ethofer T, Kardatzki B, Erb M, Scheffler K, Berg D, *et al*. Gait decline while dual-tasking is an early sign of white matter deterioration in middle-aged and older adults. Front Aging Neurosci 2022;14:934241. doi: 10.3389/fnagi.2022.934241.
61. Meder D, Herz DM, Rowe JB, Lehericy S, Siebner HR. The role of dopamine in the brain-lessons learned from Parkinson's disease. Neuroimage 2019;190:79–93. doi: 10.1016/j.neuroimage.2018.11.021.
62. Surkont J, Joza S, Camicioli R, Martin WRW, Wieler M, Ba F. Subcortical microstructural diffusion changes correlate with gait impairment in Parkinson's disease. Parkinsonism Relat Disord 2021;87:111–118. doi: 10.1016/j.parkreldis.2021.05.005.

How to cite this article: Wei X, Wang SY, Zhang MK, Yan Y, Wang Z, Wei W, Tuo HZ, Wang ZC. Alterations of diffusion kurtosis measures in gait-related white matter in the "ON–OFF state" of Parkinson's disease. Chin Med J 2025;138:1094–1102. doi: 10.1097/CM9.0000000000003486